Earthquakes and Structures, *Vol. 10, No. 4 (2016) 913-938*
DOI: http://dx.doi.org/10.12989/eas.2016.10.4.913

Seismic evaluation of RC stepped building frames using improved pushover analysis

Pradip Sarkar*[1], A. Meher Prasad[2a] and Devdas Menon[2b]

[1]*Department of Civil Engineering, National Institute of Technology Rourkela, Odisha - 769 008, India*
[2]*Department of Civil Engineering, Indian Institute of Technology Madras, Chennai - 600 036, India*

(Received April 15, 2015, Revised November 20, 2015, Accepted November 23, 2015)

Abstract. 'Stepped building' frames, with vertical geometric irregularity, are now increasingly encountered in modern urban constructions. This paper proposes a new approach to determine the lateral load pattern, considering the contributions from the higher modes, suitable for pushover analysis of stepped buildings. Also, a modification to the displacement coefficient method of ASCE/SEI 41-13 is proposed, based on nonlinear time history analysis of 78 stepped frames. When the newly proposed load pattern is combined with the modified displacement coefficient method, the target displacement for the stepped building frame is found to match consistently the displacement demand given by the time history analysis.

Keywords: stepped building; pushover analysis; lateral load pattern; displacement coefficient method; target displacement

1. Introduction

A common form of vertical discontinuity arises in multi-storeyed framed buildings from reduction of the lateral dimension along its height. This building category, known as 'stepped' building (Sarkar *et al*. 2010), is becoming increasingly popular in modern multi-storey building construction mainly because of its functional and aesthetic architecture. In particular, such a stepped-form provides for adequate daylight and ventilation for the lower storeys in an urban locality with closely spaced tall buildings. This type of building form also provides for compliance with building bye-law restrictions related to 'floor area ratio' (practice in India). Fig. 1 shows a typical example of a stepped building located in urban India (New Delhi).

Stepped buildings are characterized by staggered abrupt reductions in floor area along the height of the building, with consequent drops in mass, strength and stiffness (not necessarily at the same rate). Height-wise changes in stiffness and mass render the dynamic characteristics of these buildings different from the 'regular' building (Elnashai and Sarno 2008). The stepped building form is recognized by several design codes (IS 1893: 2002 and ASCE 7: 2010) as a typical form of vertical geometric irregularity that merits special design consideration. But, there is very limited

*Corresponding author, Associate Professor, E-mail: sarkarp@nitrkl.ac.in
[a]Professor, E-mail: prasadam@iitm.ac.in
[b]Professor, E-mail: dmenon@iitm.ac.in

http://www.techno-press.com/journals/eas&subpage=7 ISSN: 2092-7614 (Print), 2092-7622 (Online)

Fig. 1 A typical stepped building located in New Delhi, India

published literature available on the lateral load resisting behavior of stepped moment resisting frames. An extensive literature survey has revealed only four journal papers (Sarkar *et al*. 2010, Athanassiadou 2008, Karavasilis *et al*. 2008, Wood 1992) in this area. Three of these papers (Sarkar *et al*. 2010, Athanassiadou 2008, Wood 1992) deal with concrete frames, while the forth paper (Karavasilis *et al*. 2008) deals with steel frames. All of these papers conclude that the higher mode participation is significant in these buildings. One paper (Athanassiadou 2008) concludes that the conventional pushover analysis does not work for stepped building and recommends against the use of pushover analysis for such buildings.

The literature survey revealed, however, extensive research work on another category of buildings with vertical geometric irregularity, namely, 'setback buildings' (where a narrow tower projects from a wide base). Setback buildings can be considered as a special case of stepped building and the lateral load resisting behavior of setback and stepped building may be of similar nature. The research papers on setback buildings (Roy and Mahato 2013, Varadharajan *et al.* 2013a, Varadharajan *et al.* 2013b, Das and Nau 2003, Wong and Tso 1994, Sharooz and Moehle 1990, Cheung and Tso 1987) were reviewed to gain insight into the behavior of vertically irregular buildings. Most of these studies conclude that the higher mode participation is significant in these buildings. Also, the inter-storey drifts for setback buildings are reported (Das and Nau 2003) to be more in the upper floors and less in the lower floors, compared to similar regular buildings without setbacks. However, there is no published literature found on the seismic evaluation of setback building using pushover analysis.

The evaluation of the seismic performance of stepped (or setback) building may not be possible using conventional pushover analysis outlined in ASCE/SEI 41-13, because of its limitations for the structures with significant higher modes effects. Although there have been a number of efforts reported in literature (Reyes *et al*. 2015, Jiang *et al*. 2010, Dolšek and Fajfar 2005, Chopra *et al.* 2004, Chopra and Goel 2002, etc.) to extend the conventional pushover analysis procedure to include different irregular building categories, stepped and setback buildings have not been addressed in this regard so far. It is instructive to study the performance of conventional pushover analysis methodology as well as other alternative pushover methodologies available in literature

for stepped buildings and to suggest improvements suitable for stepped buildings.

In the present study, a fixed lateral load pattern is developed using the properties of the first three elastic modes for pushover analysis of stepped building. The resulting pushover curve and the hinge distribution in the stepped building frames are found to be in close agreement with the nonlinear time history analysis results. Also, a modification to the displacement coefficient method of ASCE/SEI 41-13 is proposed based on nonlinear time-history analysis results of 78 stepped building frames each subjected to twenty earthquake ground motions. When the proposed load pattern is combined with the proposed modification of the displacement coefficient method the target displacement for the stepped building frame is found to match the mean displacement demand given by the time history analyses consistently.

The plan asymmetry arising out of the vertical geometric irregularity strictly calls for three-dimensional analysis to account properly for torsion effects. This is not considered in the present study, which is limited to analysis of representative plane stepped frames to consider loading in the primary direction only.

2. Structural modelling

The present study is based on nonlinear analysis of a family of structural models representing vertically irregular multi-storeyed stepped buildings. 78 building frames representing varying degree of stepped irregularity are considered for the study. However, the results presented here are limited to 11 building frames having three different building geometries with different stepped irregularities due to the successive reduction of one bay and one step-height of one storey (S1), two storeys (S2) and three storeys (S3), at the top of the building as shown in Fig. 2. The regular frame (R), without any step, is also included for reference. Additional studies carried out on 67 building frames are available elsewhere (Sarkar 2008).

Concept of regularity index (η) is used to quantify the irregularity of the stepped frames in this study (Sarkar *et al*. 2010).

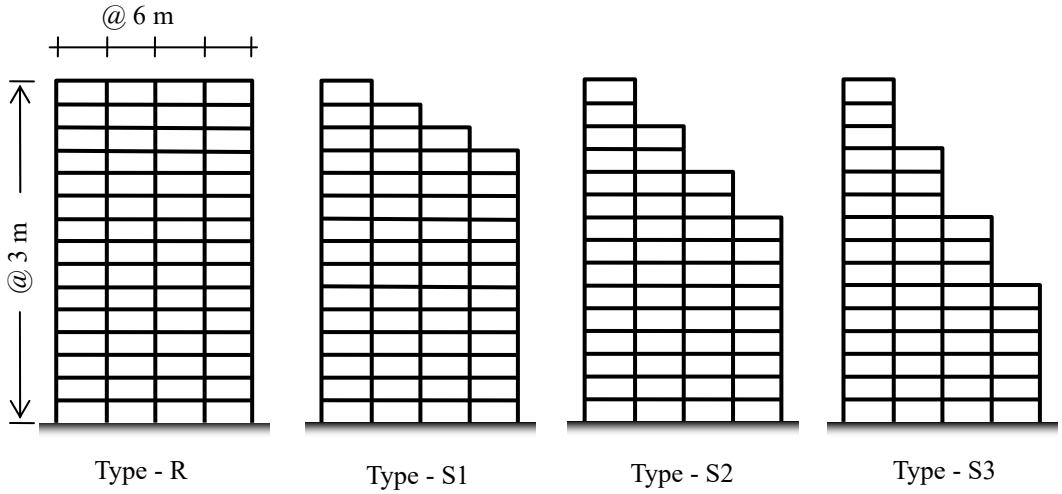

Fig. 2 Typical 15-storey building models considered for the present study

$$\eta = \frac{\Gamma_1}{\Gamma_{1,ref}} \tag{1}$$

where, Γ_1 is the 1st mode participation factor for the stepped frame under consideration and $\Gamma_{1,ref}$ is the 1st mode participation factor for the similar regular building frame without steps. All of these frames were designed as per Indian Standard IS 1893:2002 loading requirements, corresponding to the highest seismic zone (PGA=0.36 g) with the design of reinforced concrete elements conforming to IS 456:2000 and IS 13920:1993. It may be noted that in these code compliant designs, ultimate failure is likely to be caused by formation of flexural hinges, and not due to shear. All the building models considered here have four bays (in the direction of earthquake) with a uniform bay width of 6 m. It should be noted that bay width of 4 m-6 m is the usual case, especially in Indian and European practice. However, the results were checked for frames with different number of bays and it has been observed that number of bays do not affect the building response significantly. Six different height categories (6, 8, 10, 12, 15 and 18 storey) with uniform storey height of 3 m were considered for the study. These building frames include different (equal and unequal) step heights and widths.

The fundamental period (T) versus total height (H) variation of the selected frames are kept consistent with the empirical relationships proposed by Goel and Chopra (1997) as shown in Fig. 3. This figure also plots measured period data for RC moment resisting framed buildings presented in Goel and Chopra (1997). This ensure that the models selected for this study can be interpreted as being representative of general moment resisting RC frame behavior for six to eighteen-storey levels.

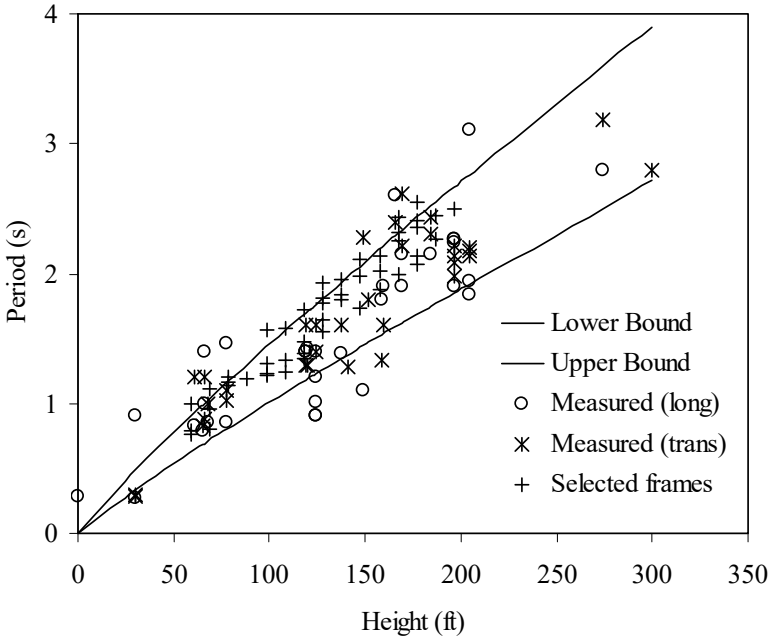

Fig. 3 Fundamental period versus height scatter of the selected frames superimposed by the empirical boundaries presented by Goel and Chopra (1997)

Table 1 Characteristics of the selected ground motion

Sl	Earthquake	Magnitude	Epicenter Distance (km)	Duration (s)	PGA (g)
1	Imperial Valley Earthquake May 18, 1940	6.9	16.9	12	0.32
2	Loma Prieta - Oakland Outer Harbour Wharf. October 17, 1989	7.1	3.5	40	0.22
3	Loma Prieta - Corralitos, Eureka Canyon Rd. October 17, 1989	7.1	7	40	0.62
4	Loma Prieta - Hollister, South Street and Pine Drive. October 17, 1989	7.1	48	60	0.38
5	Loma Prieta - Lexington Dam October 17, 1989	7.1	6.3	40	0.44
6	Northridge - Santa Monica City Hall Grounds. January 17, 1994	6.7	23	60	0.93
7	Northridge - Sylmar, County Hosp. Parking Lot. January 17, 1994	6.7	16	60	0.91
8	Northridge - Century City, Lacc North. January 17, 1994	6.7	20	60	0.27
9	Northridge - Newhall, La County Fire Station. January 17, 1994	6.7	20	60	0.63
10	Landers - Yermo, Fire Station June 28, 1992	7.3	84	80	0.25
11	Landers - Lucerne Valley June 28, 1992	7.3	42	48	0.81
12	Petrolia - Cape Mendocino April 25, 1992	7.1	8.5	60	0.59
13	Sierra Madre - Altadena, Eaton Canyon Park. June 28, 1991	5.6	12.6	40	0.45
14	Imperial Valley Earthquake - El Centro, Array 6, Huston Rd. October 15,1979	6.6	13.2	40	0.34
15	Morgan Hill - Gilroy 4, San Ysidro School. April 24, 1984	6.2	37.4	60	0.36

Commercial software SAP2000 (v.14) is used for modeling and analyzing. Standard point-plasticity approach is considered for modeling nonlinearity in the present study. Beam and column elements were modeled with flexure (M3 for beams and P-M2-M3 for columns) and shear (V2 for beams, V2 and V3 for columns) hinges at possible plastic regions under lateral load. Hinge properties are generated using modified Mander's model (Panagiotakos and Fardis 2001) of constitutive relation for concrete and Indian Standard IS 456: 2000 model for reinforcing steel. Plastic hinge length is taken as half the member overall depth for the calculation of flexural hinge property (Paulay and Priestley 1992). Detailed procedure for calculation of flexural and shear hinges can be available in literature (Sarkar 2008). To maintain the similarity, same models were used for both pushover and time-history analysis. This hinges use isotropic dissipation rule to model energy dissipation in cyclic loading. The damping matrix, in time history analysis, was calculated as a linear combination of the stiffness matrix scaled by a coefficient, and the mass matrix scaled by a second coefficient as per Rayleigh's method. These coefficients were computed

by specifying equivalent fractions of critical modal damping at two different periods. 'Hilber-Hughes-Taylor alpha' (HHT) method was used for performing direct-integration time-history analysis. This modeling approach is used by different researchers (Luca *et al*. 2014, Carvalho *et al.* 2013) for conducting nonlinear analyses. Twenty input time histories, consisting of five artificially generated accelerogram, and fifteen natural records, were employed for the dynamic analysis of the study.

Earthquake ground motions should be obtained from the past records of the region of interest for conducting nonlinear time-history analyses. Due to paucity of recorded ground motion data in Indian region fifteen natural records from United States are selected from the website of Center for Engineering Strong Motion Data (Table 1). In many cases when recorded accelerograms are not available, artificial accelerograms representative of an earthquake expected at the site are used for the nonlinear dynamic analysis. These earthquakes are generated such that if their response spectra are calculated, they will be approximately equal to a target spectrum. The artificial accelerograms can be generated from the superposition of sine waves with random phases and the resulting amplitude modulated by a smooth function to account for the transient character of the seismic motions (Vanmarcke and Gasparini 1976). An alternative method is to modify appropriately the records of historic earthquakes so that their spectra match the design spectrum (Suárez and Montejo 2005).

Five earthquake ground motion data are generated in the present study using computer software SIMQKE 2000 (Gasparini and Vanmarcke, 1976) to match the design spectrum given in Indian Standard IS 1893: 2002 (Part-1). Fig. 4 shows the acceleration response spectrum of five generated earthquakes along with the design spectrum of IS 1893: 2002. Previous literature (Fahjan and Ozdemir, 2008) show that artificial earthquake generated using SIMQKE 2000 results good estimation of nonlinear structural response.

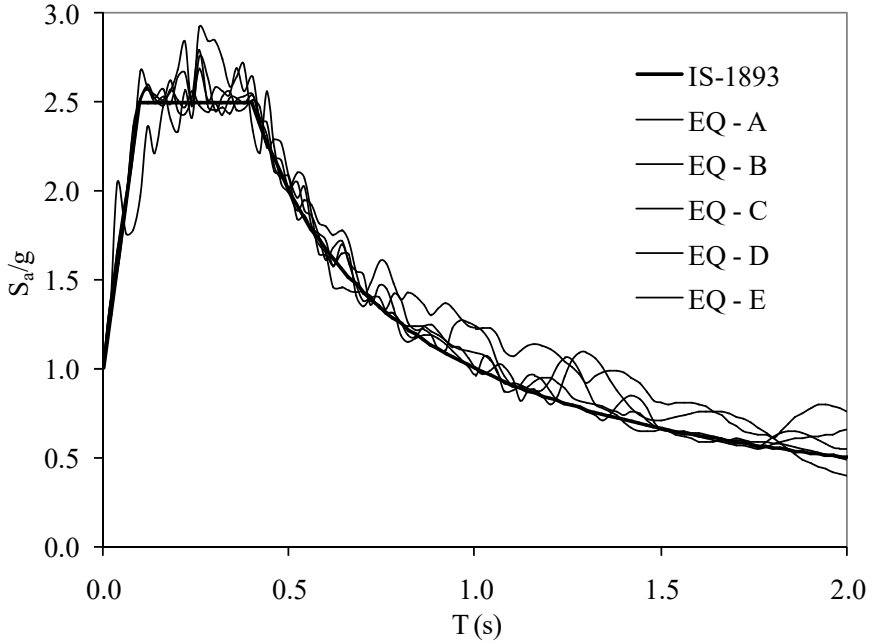

Fig. 4 Acceleration spectra for five artificial accelerograms (5% damping)

3. Lateral load distribution

To accurately evaluate the inelastic response of the structure, the prescribed earthquake load profiles must be able to describe the actual dynamic force profiles which produce maximum design values (peak values of inter-storey drift, story shear, and member forces). However, it is difficult to accurately predict such earthquake load profiles because various load profiles can develop during the nonlinear time history response of a structure. In particular, the earthquake load profiles of high-rise buildings with irregularity are complicated by the effect of higher dynamic modes. It will be appropriate to consider adaptive load pattern in pushover analysis of such buildings. However, for the present study only fixed load distribution shapes are utilised in order to keep the pushover analysis procedure simple and attractive for design office environment. A potential earthquake load profiles for the nonlinear pushover analysis of stepped buildings were developed, based on SRSS combination. The basic concept is taken from the upper-bound load profile (Jan *et al*. 2004).

The differential equations governing the elastic response of a multi-storey building subjected to horizontal earthquake ground acceleration $\ddot{u}_g(t)$ are given by

$$[m]\{\ddot{u}\}+[c]\{\dot{u}\}+[k]\{u\}=-[m]\{1\}\ddot{u}_g(t) \tag{2}$$

where $\{u\}$ is the floor displacement vector relative to the ground with $\{\dot{u}\}$ and $\{\ddot{u}\}$ representing floor velocity and acceleration vectors respectively. $[m]$, $[c]$, and $[k]$ are the mass, classical damping, and lateral stiffness matrices of the system. The solution of the above differential equation governing the response of a MDOF system to an earthquake ground motion can be expressed, using the mode superposition method, as

$$\{u(t)\}=\sum_{n=1}^{N}\{\phi_n\}q_n(t) \tag{3}$$

$$q_n(t)=\Gamma_n D_n(t)=\frac{\{\phi_n\}^T[m]\{1\}}{\{\phi_n\}^T[m]\{\phi_n\}}D_n(t) \tag{4}$$

where $\{\phi_n\}$ is the mode shape, $q_n(t)$ is the modal amplitude, Γ_n is the modal participation factor of the n^{th} mode and $D_n(t)$ is governed by the following equation of motion for a SDOF system, with n^{th} mode natural period T_n and damping ratio ξ_n, subjected to $\ddot{u}_g(t)$

$$\ddot{D}_n+\left(4\pi/T_n\right)\xi_n\dot{D}_n+\left(2\pi/T_n\right)^2 D_n=-\ddot{u}_g(t) \tag{5}$$

D_n can be alternatively obtained from elastic spectrum of the earthquake under consideration for the n^{th} mode natural period. Now, the probable maximum static forces can be expressed as

$$\{F(t)\}=[k]\{u(t)\}=\sum_{n=1}^{N}[k]\{\phi_n\}q_n(t)=\sum_{n=1}^{N}\left(2\pi/T_n\right)^2[m]\{\phi_n\}q_n(t) \tag{6}$$

Generally the modal combinations are meant for combining the peak responses from different modes. However, the forces corresponding to each mode are combined in the present study using the SRSS combination rule as the resulting force profile matches very well with the mean of the

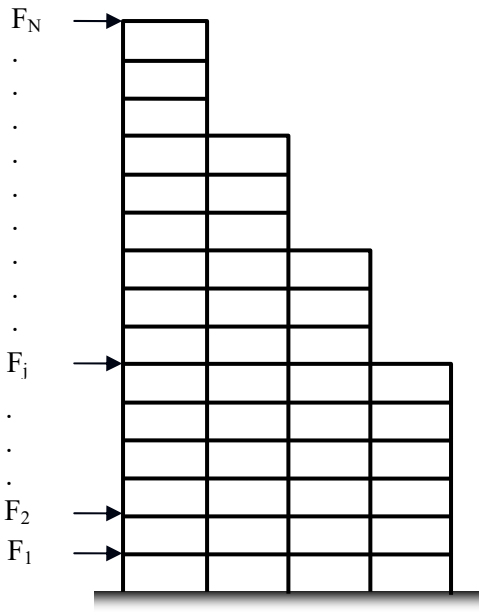

Fig. 5 Distribution of probable maximum storey force

maximum elastic storey shear distribution obtained from time history analysis. Accordingly, the probable maximum storey force at j^{th} storey (Fig. 5) can be obtained as

$$F_j = \sqrt{\left[\left(\frac{2\pi}{T_1}\right)^2 m_j \phi_{1,j} q_1\right]^2 + \left[\left(\frac{2\pi}{T_2}\right)^2 m_j \phi_{2,j} q_2\right]^2 + \ldots} \tag{7}$$

Since $\{F\}$ is a spatial vector and increases monotonically from zero in pushover analysis, Eq. (7) can simply be expressed as

$$F_j = \sqrt{\left(\frac{m_j \phi_{1,j}}{T_1^2}\right)^2 + \left(\frac{m_j \phi_{2,j}}{T_2^2}\frac{q_2}{q_1}\right)^2 + \left(\frac{m_j \phi_{3,j}}{T_3^2}\frac{q_3}{q_1}\right)^2 + \ldots} \tag{8}$$

A study has been carried out to check how many modes have significant contribution to the proposed load profile (Eq. (8)). As shown in Eq. (8), the contribution of a higher mode in comparison with the fundamental mode can be expressed as a ratio of q_i/q_1. In order to analyse the higher-mode contribution, the set of twenty earthquake ground motions were applied to the 78 designed stepped frames. Fig. 6 show the ratios obtained for 2nd, 3rd and 4th modes as a function of the fundamental time period. Similar results are available in literature (Jan *et al*. 2004) for single bay regular frames.

From these figures, it can be seen that in addition to the first mode the 2nd mode contribution is significant and to some extent the 3rd mode also contributes the structural response. The 2nd mode contribution is 10% to 40% of the fundamental mode while the 3rd mode contribution is 1% to 10% of the fundamental mode. The contribution from 4th and higher modes to the structural

response is very little and can be ignored. It is also clearly seen that higher mode contribution increases in significance when the stepped irregularity increases. Modal analysis results for 78 designed stepped frames with varying irregularity and height results that 90% of the total mass participates in first three modes and considering these three modes alone can be sufficient as given in Indian Standard IS 1893: 2002 for response spectrum analysis.

A plot of the lateral load distribution for a typical 15 storey stepped frame (S3-15) as per Eq. 8 considering only first mode along with combinations of first two, three and four modes is presented in Fig. 7. The abscissa of this figure presents the 'load ratio' which is defined as the ratio of storey force to the corresponding base shear force. This figure shows that after third mode, the load shape is almost stationary and there is no significant effect on the load profile from fourth and higher modes. Hence, the first three modes are considered to calculate the proposed lateral load distribution for pushover analysis of stepped building as follows

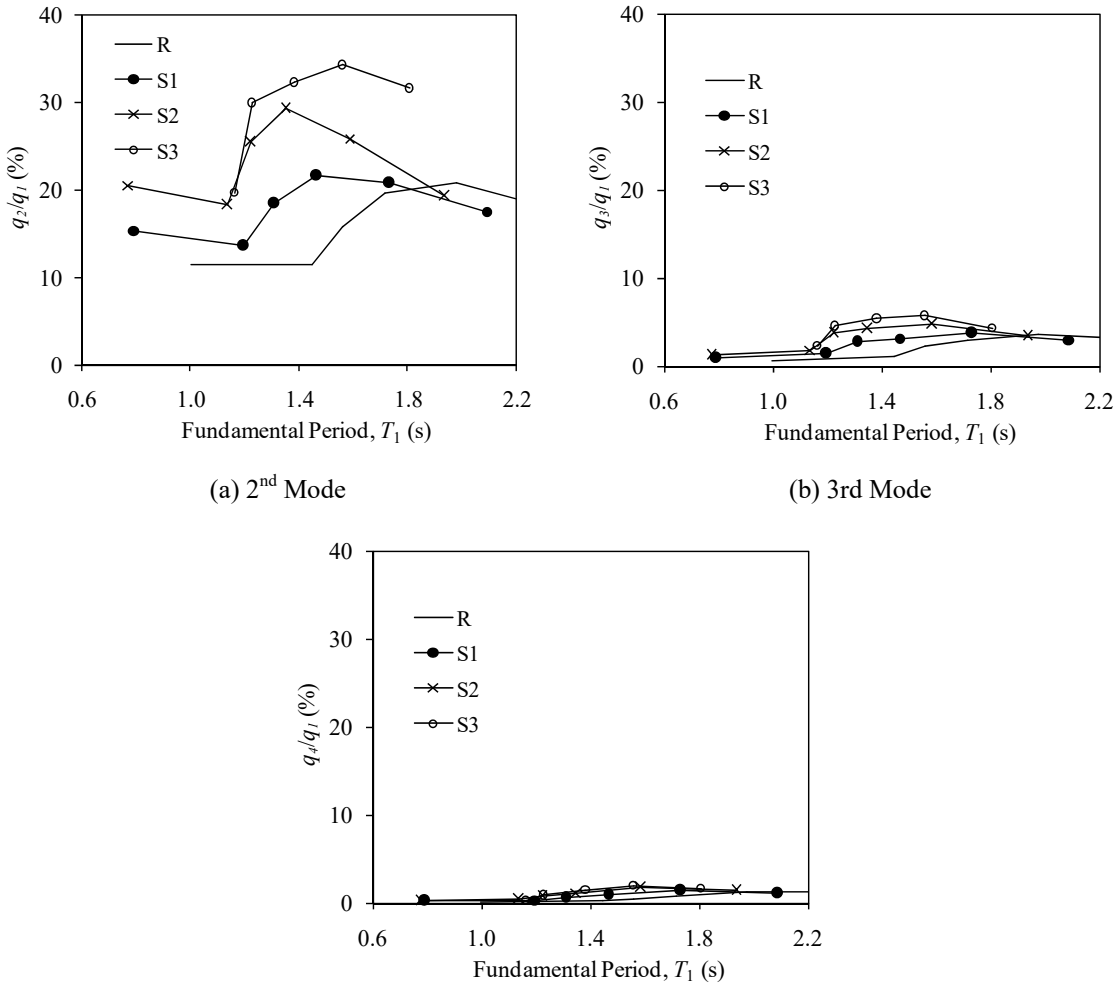

(a) 2nd Mode

(b) 3rd Mode

(c) 4th Mode

Fig. 6 Higher mode contribution ratio as a function of fundamental period

$$F_j = \sqrt{\left(\frac{m_j \phi_{1,j}}{T_1^2}\right)^2 + \left(\frac{m_j \phi_{2,j}}{T_2^2}\frac{q_2}{q_1}\right)^2 + \left(\frac{m_j \phi_{3,j}}{T_3^2}\frac{q_3}{q_1}\right)^2} \tag{9}$$

Fig. 8 presents the comparison of the proposed load profile with the mean maximum story shear profile obtained from linear time history analyses for three typical stepped frames. The figure shows that the proposed lateral load profile fairly matches closely with the storey shear profile. This is to be noted that load pattern proportional to the story shear distribution is recommended in FEMA 356 (2000) for pushover analysis when the fundamental period of the building exceeds one second.

FEMA 356 (2000) recommends the adoption of two load profiles, one each from the following two groups: Group-I (a) design code specified load distribution for equivalent static analysis, (b) fundamental mode shape and (c) storey shear profile obtained from response spectrum analysis and Group-II (a) uniform distribution and (b) adaptive distribution. The primary recommendation of ASCE/SEI 41-13 for load vector is to use the first mode shape. However, ASCE/SEI 41-13 recognises other load patterns given in FEMA 356 (2000). In the present study, the following load profiles are studied and compared: (i) equivalent static load distribution based on Indian Standard IS 1893:2002 (IS 1893), (ii) fundamental mode shape (Mode-1), (iii) mass proportional uniform distribution (UNI), (iv) load profile for upper bound pushover analysis (UBPA) and (v) proposed profile based on Eq. (9). IS 1893:2002 (Part-1) recommends a parabolic load distribution pattern for equivalent static analysis of multi-storeyed framed building as follows

$$F_j = \frac{W_i h_i^2}{\sum_1^N W_i h_i^2} V_B \tag{10}$$

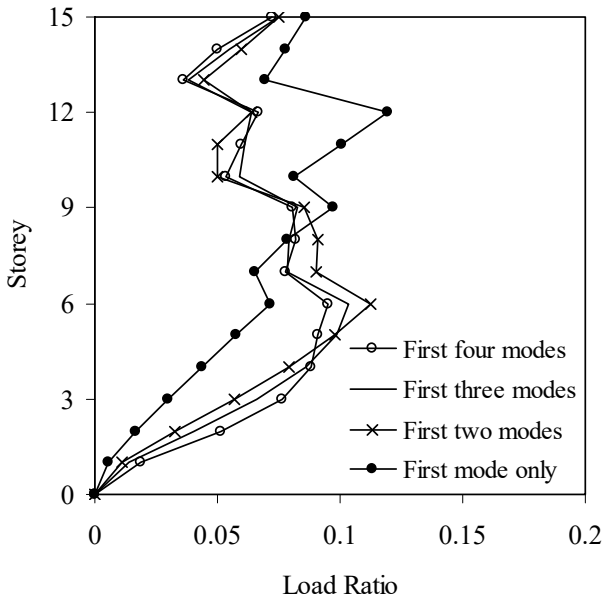

Fig. 7 Lateral load distribution for stepped frame S3-15

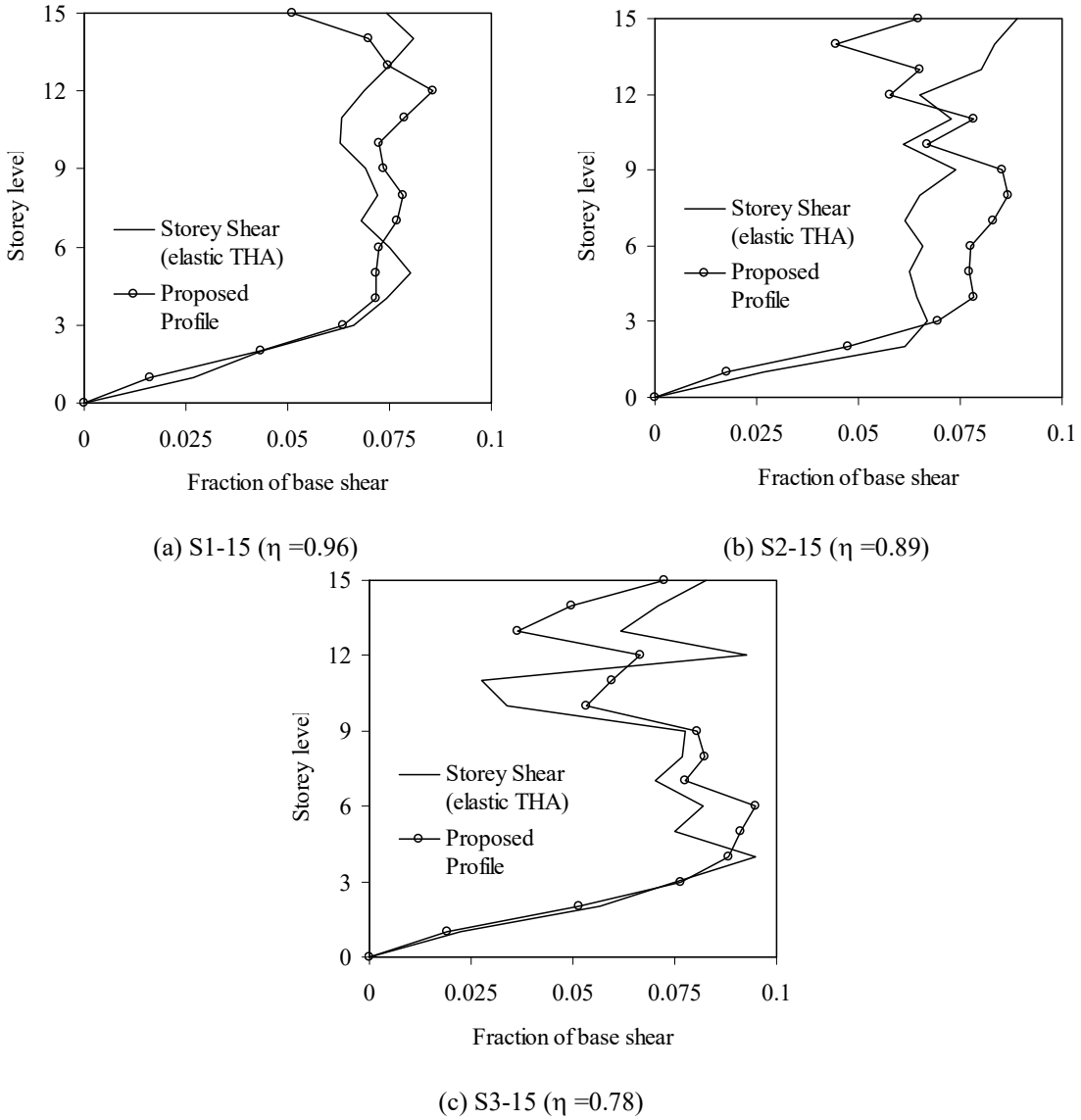

(a) S1-15 (η =0.96)

(b) S2-15 (η =0.89)

(c) S3-15 (η =0.78)

Fig. 8 Comparison of the proposed load profile with the mean of the maximum storey shear profile for typical 15-storey frames

Where, W_i and h_i are the lumped weight and height (from the ground level) of i'th storey respectively, N is the total number of the storeys and V_B is the design base shear. Fig. 9 presents the comparison of the proposed lateral load profiles with some of the existing load profiles available for pushover analysis.

The figure shows that the proposed profile adds more loads in the lower storeys and reduces load in the upper stories when compared to the fundamental mode shape and code-based load profile. The mass and stiffness of the stepped buildings get reduced at the upper floors compared to the lower floors. Both of the reduced mass and reduced stiffness are responsible for attracting

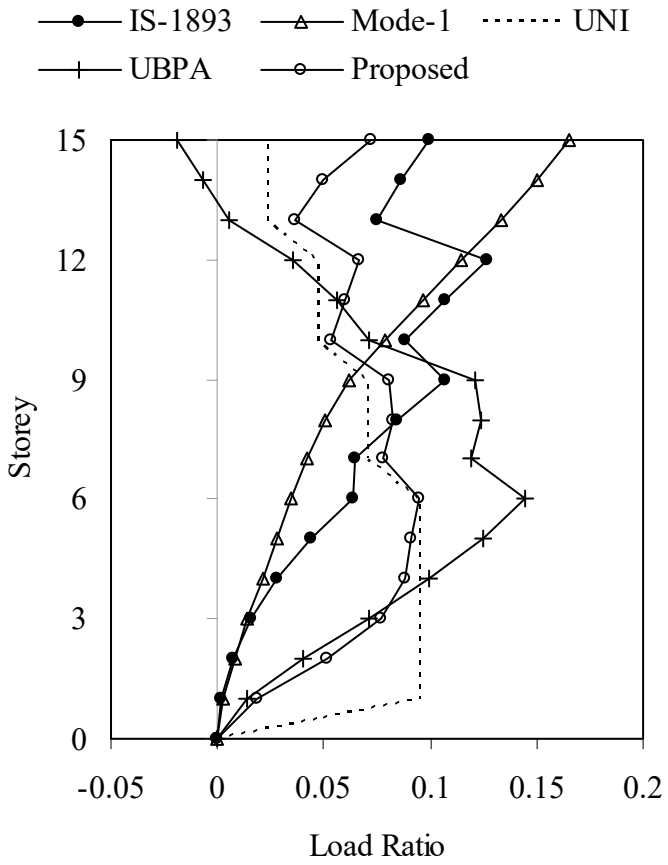

Fig. 9 Proposed lateral load profile with other existing load profiles for stepped frame S3-15

less seismic forces at the upper floors compared to similar regular buildings without steps. This is reflecting in proposed lateral load profile. Studies carried out on other frames with different heights, widths and irregularity shown similar trends. Also, this figure shows that the proposed load profile is quite close to the mass-proportional uniform load profile.

4. Estimation of target displacement

A comparative evaluation of different methods available for estimating target displacement from pushover analysis shows that all of these procedures perform well for regular building frames when compared with the results of nonlinear time history analyses. However, previous studies (Sarkar 2008) show that in case of stepped frame the displacement coefficient method of ASCE/SEI 41-13, Modal (Chopra and Goel 2002) and modified modal (Chopra *et al.* 2004) pushover analyses underestimate the target displacements whereas capacity spectrum method of ATC 40 (1996) overestimates target displacement. This section devotes to develop an improvement to the displacement coefficient method of ASCE/SEI 41-13 for its application to the stepped buildings as this method is the most popular in practice.

The displacement coefficient method of ASCE/SEI 41-13 primarily estimates the elastic displacement of an equivalent single degree of freedom (SDOF) system assuming effective linear properties and damping for the ground motion excitation under consideration. Then it estimates the total maximum inelastic displacement response of the building at roof by multiplying with a set of displacement coefficients. The expected maximum roof displacement of a building (target displacement) under the selected seismic ground motion for a particular performance level as per displacement coefficient method (ASCE/SEI 41-13) is expressed as

$$\delta_t = C_0 C_1 C_2 S_a \frac{T_e^2}{4\pi^2} \tag{11}$$

Here, the coefficient C_0 is to relates spectral displacement of an equivalent SDOF system to the exact roof displacement of the building (Multi-degree of freedom system), C_1 relates the expected maximum inelastic displacements to displacements calculated for linear elastic response and C_2 represents the effect of pinched hysteretic shape, stiffness degradation and strength deterioration. T_e is the effective fundamental period in the direction under consideration and S_a is the spectral acceleration at the effective fundamental period and damping in the direction under consideration.

Change in building geometry due to the steps will affect C_0 significantly whereas it is likely to have very little influence on the C_1 and C_2 factors. As per ASCE/SEI 41-13, the values of C_0 factor for shear buildings depend only on the number of storeys and the lateral load pattern used in the pushover analysis. Table 2 presents the values of C_0 provided by the ASCE/SEI 41-13 for shear buildings. Generally, stepped buildings are more than five storeys tall in practice and the C_0 factor, as per ASCE/SEI 41-13, is constant for buildings with five or more storeys. To assess the applicability of the values of C_0 factor given in ASCE/SEI 41-13, linear time history analyses of 78 selected stepped frames has been carried out for twenty selected earthquake ground motions, scaled for PGA=0.36 g. The mean value of the maximum roof displacement of each frame and the mean value of spectral displacement of corresponding equivalent SDOF system for all the 20 earthquakes are calculated. The equivalent period (T_e) can be generated graphically from the base shear versus roof displacement curve obtained using the proposed load profile (Eq. (9)) as per ASCE/SEI 41-13. The elastic spectral displacement corresponding to this period is calculated directly from the response spectrum representing the seismic ground motion under consideration for a specified damping ratio (5%).

Fig. 10 shows the results obtained for different stepped frames. Two lines representing the C_0 values given by ASCE/SEI 41-13 for triangular load pattern (C_0=1.3) and uniform load pattern (C_0=1.2) are also presented. This figure shows that, for most of the cases, C_0 values do not match with the ASCE/SEI 41-13 recommendation. For regular frame, the deviation is less but as the

Table 2 Values of C_0 factor for shear building as per ASCE/SEI 41-13

Number of storeys	Triangular Load Pattern	Uniform Load Pattern
1	1.0	1.0
2	1.2	1.15
3	1.2	1.2
5	1.3	1.2
10+	1.3	1.2

irregularity increases the deviation tends to increase. Also, for the lower storey frames the deviation from the ASCE/SEI 41-13 values is less compared to the higher storey frames. This indicates that the ratio of elastic roof displacement for an exact MDOF frame to the elastic spectral displacement for equivalent SDOF system increases with the increase in the number of storeys (building height) and with decrease in regularity index (i.e., increase in irregularity). It means ASCE/SEI 41-13 specified values for C_0 may work for low-rise regular buildings but for high-rise regular buildings and all stepped buildings the ASCE/SEI 41-13 values are less than the actual values.

Fig. 11 plotted to understand the effect of number of bays in a building (plan dimension) on C_0-factor. This figure presents the typical variation of C_0 value with respect to number of bays when height and regularity index are constant. It shows that C_0 factor has hardly any dependence on the bay numbers (plan dimensions). Therefore, the C_0 factor can be considered as a function of

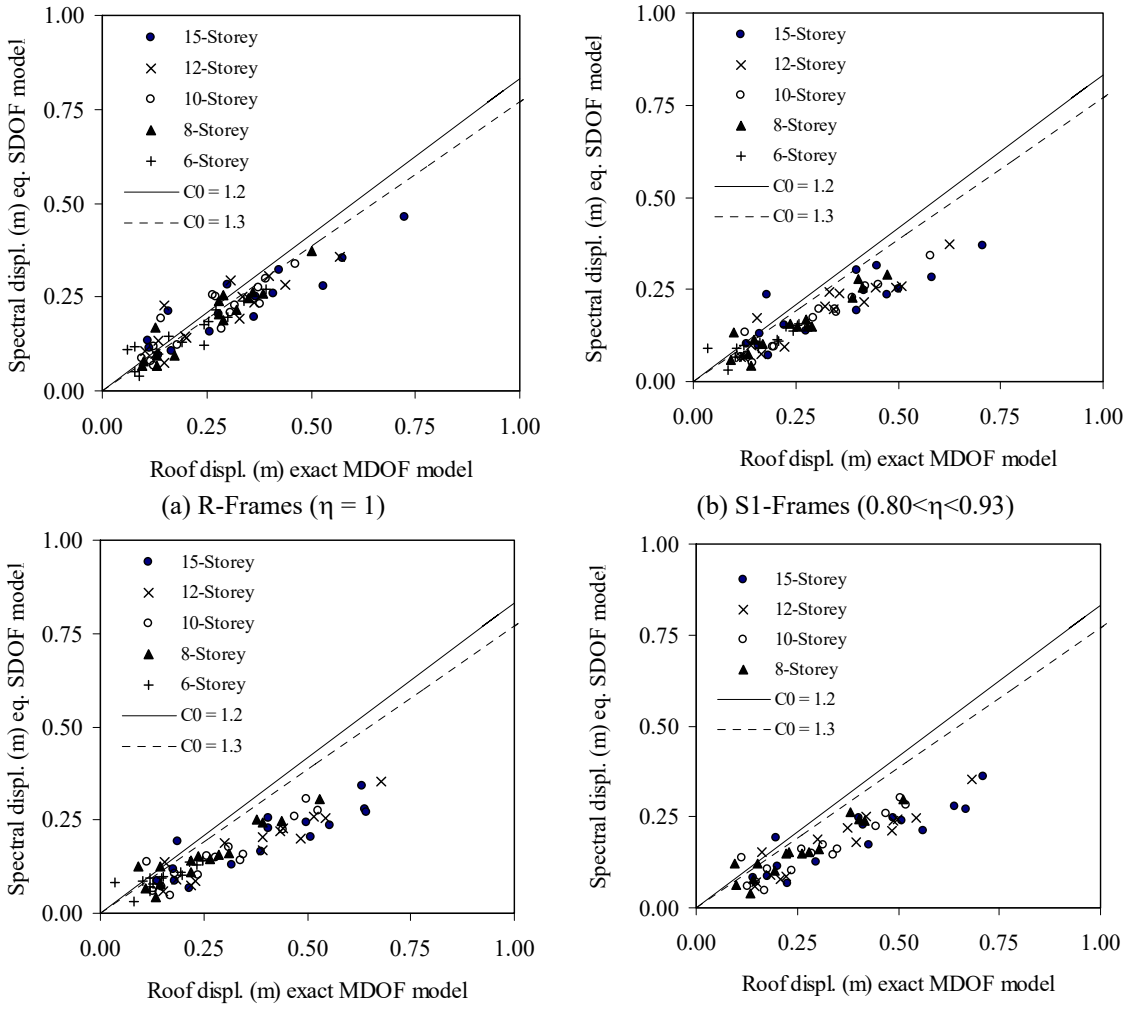

(a) R-Frames (η = 1)

(b) S1-Frames (0.80<η<0.93)

(c) S2-Frames (0.66<η<0.85)

(d) S3-Frame (0.61<η<0.76)

Fig. 10 Correlation of time history response for stepped frames

regularity index (η) and building height (h) only. Figs. 12 and 13 present the typical variation of C_0 value with respect to overall frame height and regularity index respectively.

Based on all the data developed for 78 building frames, a nonlinear regression analysis has been carried out and the following empirical equation has been arrived at for calculating the value of C_0 factor

$$C_0 = 1.5 + 0.5\eta(1-\eta)\left(\frac{h}{10} - 0.4\right) \tag{12}$$

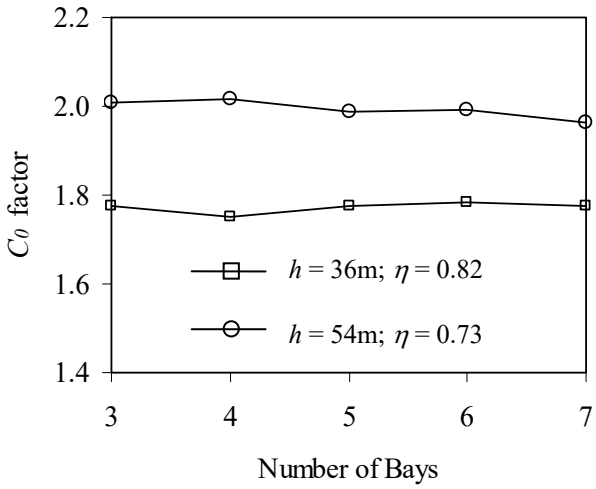

Fig. 11 Variation of C_0 factor with respect to number of bays

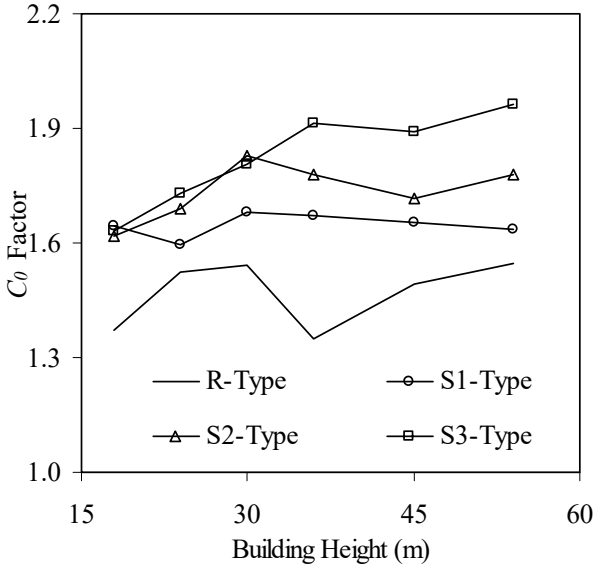

Fig. 12 Variation of C_0 factor with respect to frame height

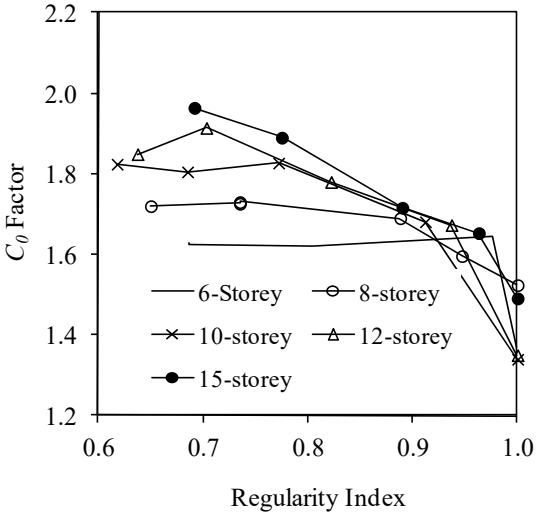

Fig. 13 Variation of C_0 factor with respect to regularity index

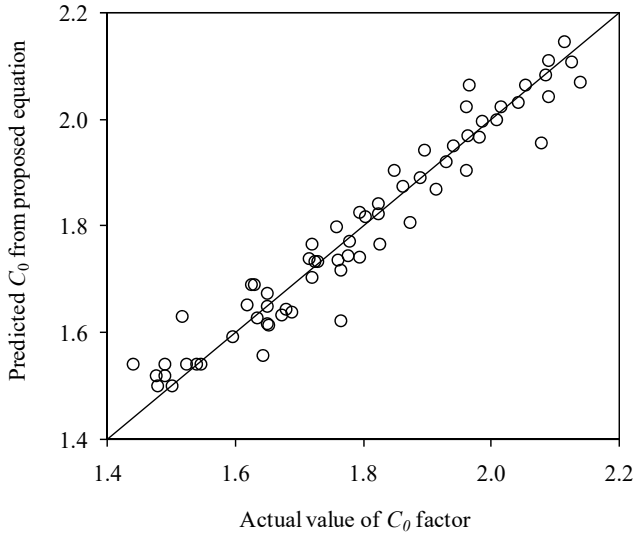

Fig. 14 Correlation between 'predicted' and 'exact' value of C_0 factor

where η=regularity index and h=building height (in m). Fig. 14 presents the correlation between the C_0 factor calculated using Eq. (12) and the actual C_0 factor obtained from the time history analysis. The average ratio of predicted to actual C_0 factor for 78 samples is 1.001 with a correlation coefficient between actual and predicted C_0 factor is 0.95.

5. Proposed procedure for pushover analysis of stepped building

Summarised below are a series of steps to be followed for the proposed pushover analysis

procedure for stepped buildings.

Perform an eigenvalue analysis and find out the natural periods and mode shapes of the structure.

Use the elastic response spectrum of the selected earthquake to determine the 2nd mode and 3rd mode contribution ratio, (q_2/q_1) and (q_3/q_1) respectively, as given by the following expression:

$$\frac{q_n}{q_1} = \frac{\Gamma_n D_n}{\Gamma_1 D_1}$$

where Γ_n (n=2 and 3) is the modal participation factor and D_n (n=2 and 3) is the displacement obtained from the elastic displacement response spectrum for n^{th} mode period.

Determine the lateral load distribution (height-wise) for pushover analysis using the following equation for probable maximum storey force at j^{th} storey

$$F_j = \sqrt{\left(\frac{m_j \phi_{1,j}}{T_1^2}\right)^2 + \left(\frac{m_j \phi_{2,j}}{T_2^2}\frac{q_2}{q_1}\right)^2 + \left(\frac{m_j \phi_{3,j}}{T_3^2}\frac{q_3}{q_1}\right)^2}$$

where T_n and $\phi_{i,j}$ (n=1, 2 and 3) are the natural period and j'th floor mode shape value for the n^{th}-mode; m_j is storey mass at j'th floor.

Carry out the pushover analysis with above lateral load profile $\{F_j\}$ till the collapse mechanism is formed and evaluate the properties of effective SDOF system from the associated capacity curve as per ASCE/SEI 41-13.

Determine the target roof displacement as given by the following relationship:

$$\delta_t = C_0 C_1 C_2 S_d = C_0 C_1 C_2 \frac{T_e^2}{4\pi^2} S_a$$

where $C_0 = 1.5 + 0.5\eta(1-\eta)\left(\frac{h}{10} - 0.4\right)$ and all other coefficients are to be calculated as per ASCE/SEI 41-13. S_d and S_a are spectral displacement and spectral acceleration of the ground motion under consideration corresponding to the period of effective SDOF system, T_e.

Determine the seismic demands of a given structure by pushover analysis with a lateral load profile $\{F_j\}$ and the target displacement δ_t.

The flowchart presented in Fig. 15 illustrates the main steps to follow for the proposed pushover analysis procedure.

6. Performance of the proposed pushover analysis procedure

All the selected frames with varying irregularity and height were analysed using the proposed pushover analysis procedure and other alternative procedures available in literature. The pushover analysis results are then compared with the nonlinear time history (NLTHA) analysis results for twenty selected earthquake ground motions. These ground motion records are scaled for various PGA levels ranging from 0.18 g to 0.72 g to force the structural collapse and to get an envelope for the base shear versus roof displacement curve up to the collapse.

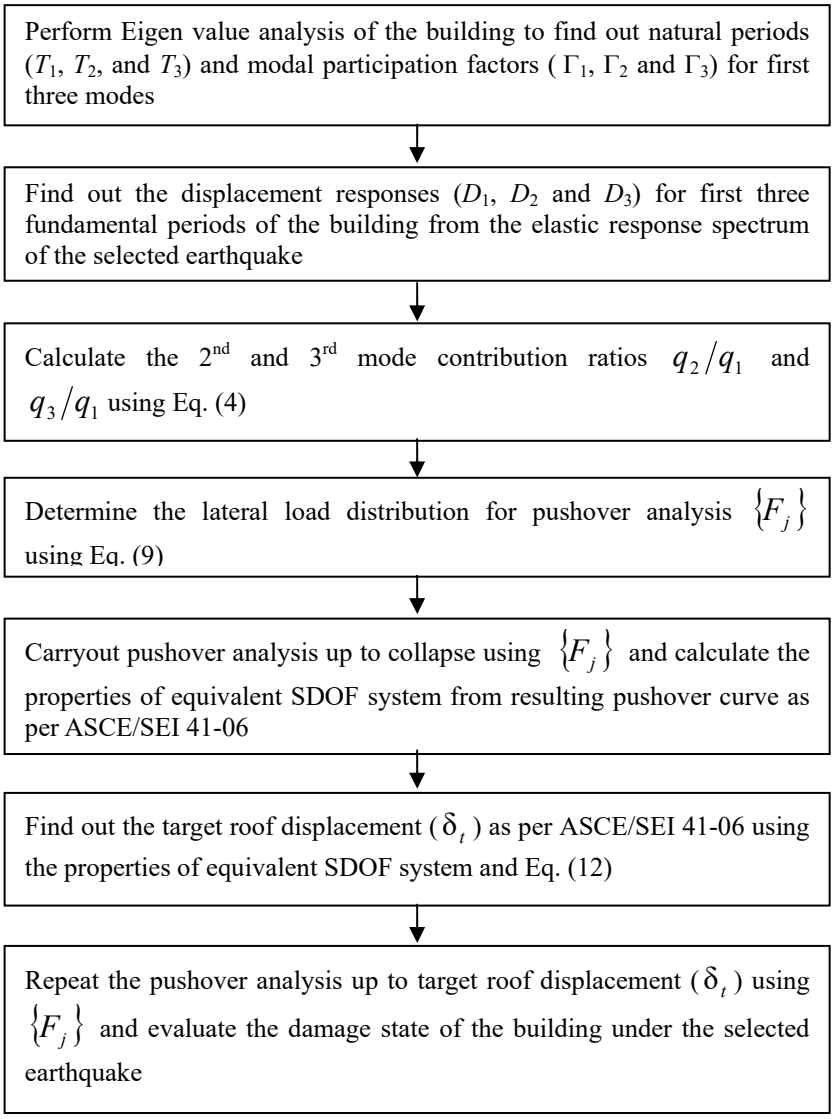

Fig. 15 Flowchart of the proposed pushover analysis procedure for stepped building

6.1 Pushover curve

Fig. 16 presents the comparison of typical pushover curves using the proposed lateral load profile as well as few existing load profiles available for pushover analysis, i.e., uniform distribution (UNI), fundamental mode shape (Mode-1), code-based load pattern (IS 1893), and load profile for upper bound pushover analysis (UBPA) for 15-storey building frames. This figure also presents the base shear versus roof displacement envelops obtained from nonlinear time history analysis (NLTHA). Envelopes are preferred here instead of the mean values to represent results of NLTHA because the envelopes indicate the base shear and roof displacement capacities

better than what mean values do. Also, it is numerically easier to plot the envelop curves from NLTHA results and compare them with the corresponding pushover curves.

Use of two lateral load patterns (mass proportional uniform distribution and code-based distribution or fundamental mode shape or storey shear distribution from response spectrum analysis) was intended by ASCE/SEI 41-13 to bind the range that may occur during actual dynamic response. This figure shows that for regular building (η=1.0) and less irregular stepped buildings ($\eta \geq 0.9$) the two load patterns from ASCE/SEI 41-13 (uniform distribution and fundamental mode shape) indeed represent the upper bound and the lower bound of the nonlinear time history analysis results. But this assumption does not hold good for stepped frames with less regularity index (i.e., frames with high irregularity). The results shown in Figs. 16 (c) and 16 (d) reveal that the two load patterns recommended by ASCE/SEI 41-13 cannot bind the solution for

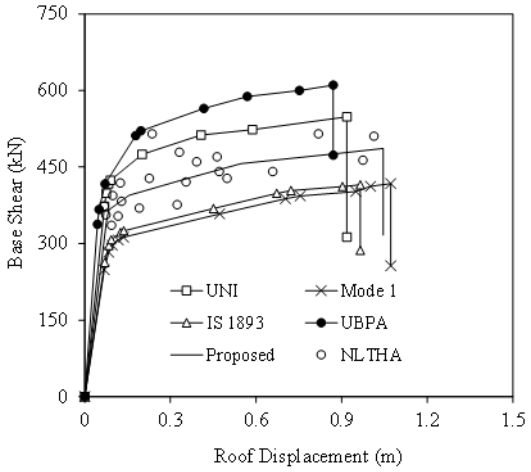

(a) Frame R-15, η = 1

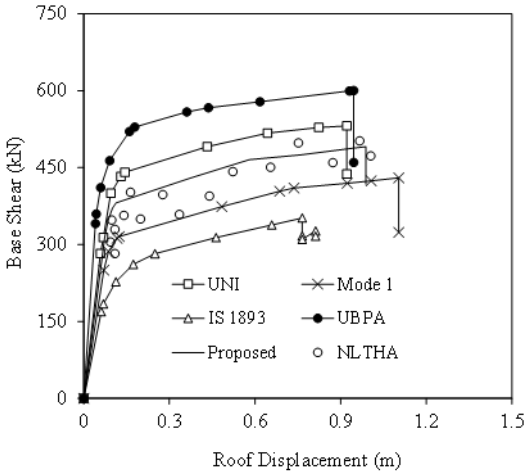

(b) Frame S1-15, η = 0.96

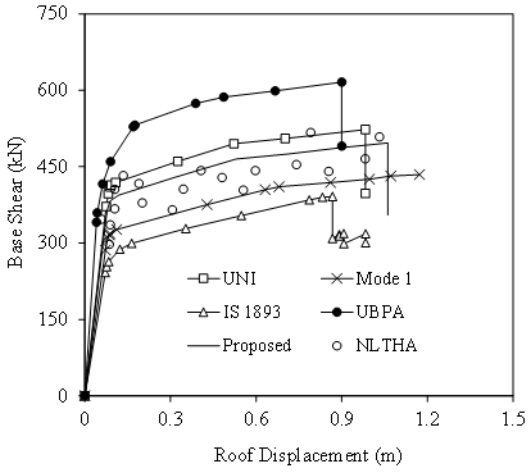

(c) Frame S2-15, η = 0.89

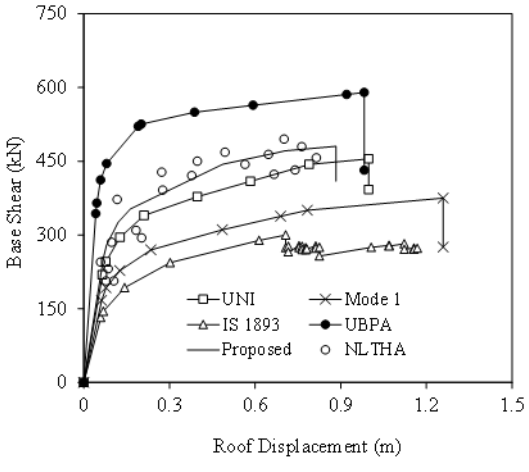

(d) Frame S3-15, η = 0.78

Fig. 16 Pushover curve for 15-storey stepped frame

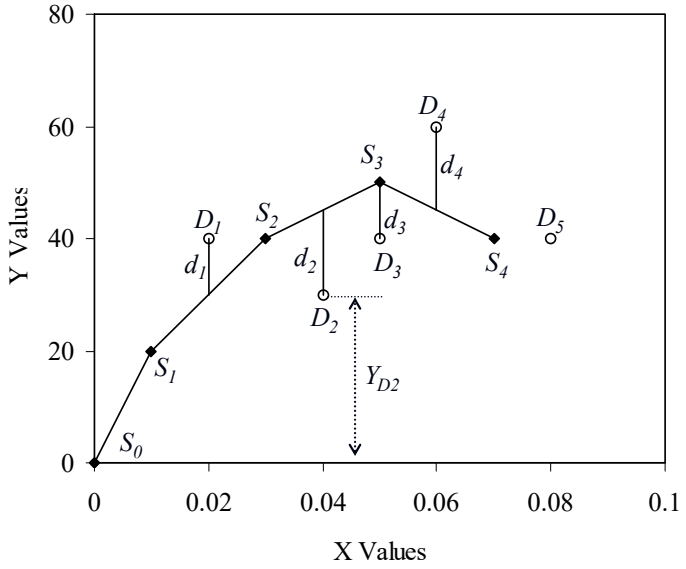

Fig. 17 Definition of pushover curve error index (Papanikolaou 2005)

the stepped building with less regularity index ($\eta \leq 0.8$). Time history envelops show greater strength than that predicted by the pushover analysis using uniform load pattern for stepped building with less regularity index. This is due to the fact that the earthquake forces at the upper storeys of stepped buildings are less compared to the lower storeys due to the relatively lesser mass and lesser stiffness at that level. The proposed load distribution, which has more load intensity at the lower part of the frame compared to the upper part, reflect the time history analysis results most closely. It can be seen through Fig. 16 that pushover analysis with the proposed lateral load profile can predict the results that match best with the NLTHA results.

Pushover curve error index (E_{pc}) is used as a measure of the discrepancy between the pushover analysis and nonlinear time history analysis in terms of base shear versus roof displacement relation (Papanikolaou *et al*. 2005). It is numerically simple and very efficient to define the difference between the ordinates of a pushover curve and the base shear versus roof displacement envelop obtained from the nonlinear time history analysis for the same structural model. Fig. 17 shows the pushover curve S_0-S_4 and the set of envelop points (D_1-D_5) obtained from nonlinear time history analysis for a typical building frame. The coordinates of the vertical projection of each time history analysis point on the pushover curve are calculated by linear interpolation between neighboring pushover points. Points with no projections (like D_5 in Fig. 17) are ignored. The pushover curve error index (E_{pc}) is calculated using the following equation

$$E_{PC} = \sqrt{\frac{1}{N}\sum_{1}^{N}\left(\frac{d_i}{Y_{Di}}\right)^2} \tag{12}$$

where d_i is the vertical projection of the i^{th} time history analysis point on the pushover curve, Y_{Di} is the Y-coordinate of i^{th} time history analysis point and N is the total number of points considered. A value of pushover curve error index approaching to zero implies high accuracy in the pushover

Table 3 Pushover curve error index

FRAME	Regularity Index (η)	UNI	MODE-1	IS-1893 distribution	UBPA	Proposed
R-15	1.00	0.18	0.20	0.20	0.22	0.08
S1-15	0.96	0.16	0.13	0.17	0.24	0.10
S2-15	0.89	0.15	0.11	0.19	0.23	0.11
S3-15	0.78	0.11	0.22	0.20	0.19	0.08
R-10	1.00	0.21	0.20	0.18	0.31	0.08
S1-10	0.91	0.20	0.22	0.23	0.32	0.09
S2-10	0.77	0.18	0.22	0.22	0.30	0.10
S3-10	0.69	0.10	0.23	0.23	0.28	0.11
R-6	1.00	0.23	0.19	0.17	0.31	0.09
S1-6	0.84	0.22	0.20	0.21	0.33	0.11
S2-6	0.69	0.16	0.20	0.20	0.32	0.08
Mean Error	-	0.17	0.19	0.20	0.28	0.09

analysis results (proximity to the time history analysis results). Table 3 presents the pushover curve error index for different frames for various load patterns used in pushover analysis. The table shows that proposed profile predicts results with more accuracy compared to the other existing lateral load profiles.

The maximum displacement undergone by the building frame at collapse is obtained from pushover analyses with different load patterns and compared with the mean value of the maximum displacements undergone by the same structure in nonlinear time history analyses for twenty different earthquake ground motions. It is found that uniform (UNI) and UBPA load patterns almost always under-estimate the maximum displacement the structure undergoes before collapse. However, for frames with higher irregularity (S3-type) and higher frame height (more than fifteen storey), both of these two load patterns overestimate the maximum displacement capacity. The load pattern corresponding to the fundamental mode shape (Mode-1) and uniform (UNI) load pattern result in a good estimation of maximum displacement for frames with less irregularity or less height (variation is within 20% for R, S1 and S2 type frames), while the UBPA load pattern shows a very high variation from the mean time history analysis results for almost all the cases (variation is up to 50%). The proposed load pattern estimates the maximum roof displacement of stepped frames for any height category with less than 10% error.

Similarly, the base shear capacity values of the frame estimated by pushover analyses with different load patterns are compared with the mean value of base shear capacity of the same structure as obtained from nonlinear time history analysis. It is found from the study that the estimation of base shear capacity using UBPA load pattern is the poorest among all others. It highly over-estimates the base shear capacity (up to 30%). It is noticed that the pushover analysis with load profile corresponding to the fundamental mode shape always underestimates the base shear capacity. Pushover analysis with mass proportional uniform load pattern is found unable to predict the upper bound of the base shear capacity for frames with more irregularity (S2 and S3 types). However, uniform load pattern is found to represent the upper bound estimation of the base shear capacity for the frames with less irregularity (R and S1 types). The proposed load profile

performs better than other lateral load profiles studied here for all the building frames. It slightly underestimates the base shear capacity (with a variation up to 10%), which is conservative.

6.2 Estimation of target displacement

Target displacement was calculated for all the building frames studied here using displacement coefficient method of ASCE/SEI 41-13, modal pushover analysis (MPA), modified modal pushover analysis (MMPA), upper bound pushover analysis (UBPA) and proposed method for 0.36 g design spectrum and compared with the mean displacement demand obtained from nonlinear time history analysis for twenty earthquake ground motion with normalized PGA (0.36 g). Eq. (11) is used to calculate the target displacement for ASCE/SEI 41-13. The required displacement coefficients are obtained from ASCE/SEI 41-13 and the effective fundamental period (T_e) is computed from pushover analysis based on the load pattern as per IS 1893:2002. A similar equation given by Jan *et al*. (2004) is used to calculate the target displacement for UBPA. For, MPA the pushover analyses are carried out separately for each significant mode (1^{st}, 2^{nd} and 3^{rd}) and the contribution of individual modes are combined using SRSS rule to calculate target displacement (Chopra and Goel 2002). This procedure involves inelastic response history analysis of equivalent SDOF systems. Target displacement calculated for MMPA is computed by combining the inelastic response of first mode and the elastic response of higher modes (Chopra *et al*. 2004). Table 4 presents the estimated values of target displacement for each frame. Values in bracket show the ratio of 'estimated (pushover analysis)' and 'exact (nonlinear time history analysis)' value of target displacements. It can be seen from Table 4 that the displacement coefficient method (ASCE/SEI 41-13), MPA, and MMPA always underestimate the target displacement for all the cases studied here. Estimation of target displacement using UBPA is found to be better than all the existing methods. The proposed method estimates target displacement very close to the time history analysis result (average ratio=1.04) with a coefficient of variation of 3%. An interesting observation here is that all the methodologies studied here result in reasonably accurate estimation of target displacement for regular frames. However, for the stepped frame, all of these methods except UBPA failed to give accurate estimation.

6.3 Distribution of hinges at collapse

Distribution of hinges at collapse is one of the important outputs of pushover analysis. It reveals the possible failure mechanism for the structure. The pattern of hinge formation is solely dependent to lateral load profile used in the pushover analysis.

Fig. 18 presents the hinge distribution in a typical stepped frame (S3-15) as obtained from pushover analysis with conventional code-based load pattern and that with the proposed lateral load pattern. This figure also presents the hinge distribution for the same frame obtained from time history analysis for a typical earthquake ground motion (Elcentro). This is to be noted that 'CP' in Fig. 18 indicates 'Collapse Prevention' performance limit state of failure defined for flexural plastic hinges as per FEMA 356 (2000). The figure clearly shows that, in pushover analysis, when code-based load pattern is used, all of the column hinges are concentrated at the upper floors near the steps, while the beam hinges are well distributed. It cannot predict the possible failure mechanism at the ground floor columns, which is indicated in the time history analyses results. Since code-based load pattern has more lateral force intensity at the upper storey level, the flexural demand in the upper floor columns reach their capacity much before the ground floor columns.

Table 4 Estimated value of target displacement, mm (ratio of estimated to exact target displacement)

Frame	ASCE/SEI 41	MPA	MMPA	UBPA	Proposed	NLTHA
R-15	227 (0.83)	235 (0.86)	232 (0.85)	280 (1.03)	279 (1.03)	272 (1.0)
S1-15	183 (0.69)	209 (0.79)	205 (0.77)	253 (0.95)	267 (1.01)	265 (1.0)
S2-15	150 (0.63)	172 (0.72)	169 (0.71)	235 (0.98)	244 (1.02)	239 (1.0)
S3-15	127 (0.64)	137 (0.70)	133 (0.68)	220 (1.12)	203 (1.03)	197 (1.0)
R-10	174 (0.92)	182 (0.96)	179 (0.95)	195 (1.03)	203 (1.07)	189 (1.0)
S1-10	140 (0.79)	148 (0.84)	145 (0.82)	168 (0.95)	174 (0.98)	177 (1.0)
S2-10	104 (0.75)	112 (0.81)	108 (0.78)	164 (1.19)	145 (1.05)	138 (1.0)
S3-10	95 (0.61)	101 (0.65)	97 (0.62)	152 (0.97)	164 (1.05)	156 (1.0)
R-6	163 (0.89)	171 (0.93)	169 (0.92)	166 (0.91)	193 (1.05)	183 (1.0)
S1-6	139 (0.89)	143 (0.91)	138 (0.88)	134 (0.85)	168 (1.07)	157 (1.0)
S2-6	92 (0.62)	103 (0.69)	101 (0.68)	102 (0.68)	163 (1.09)	149 (1.0)
Avg.	(0.75)	(0.81)	(0.79)	(0.97)	(1.04)	(1.0)
COV (%)	(15.91)	(13.06)	(13.62)	(13.89)	(2.99)	-

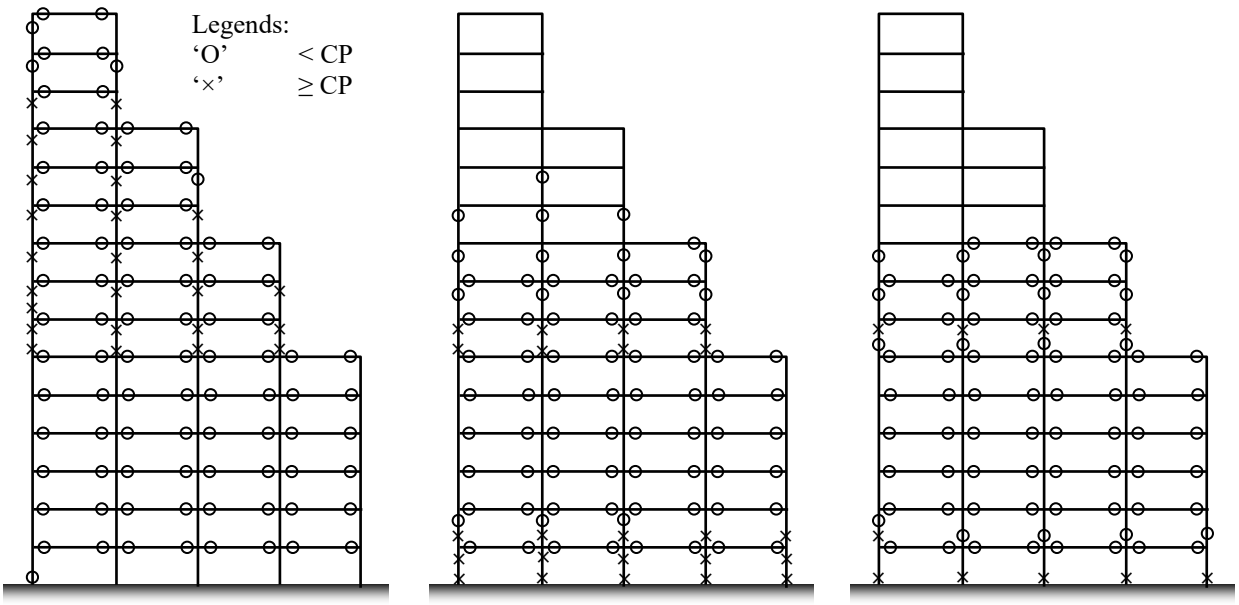

(a) PA using code-based load pattern (b) PA using proposed load pattern (c) NLTHA for Elcentro ground motion

Fig. 18 Distribution of hinges at collapse for 15 storey stepped frame (S3-15)

However, the proposed load pattern reveals the possibility of hinges forming in the ground floor columns also, as proved by the time history analysis. The same can be observed from displacement and drift profile of stepped frames at collapse. Fig. 19 presents the displacement and drift profile at collapse for a typical fifteen-storey stepped frame (S2-15) as obtained from pushover analyses with different lateral load patterns along with mean displacement and drift profile obtained from

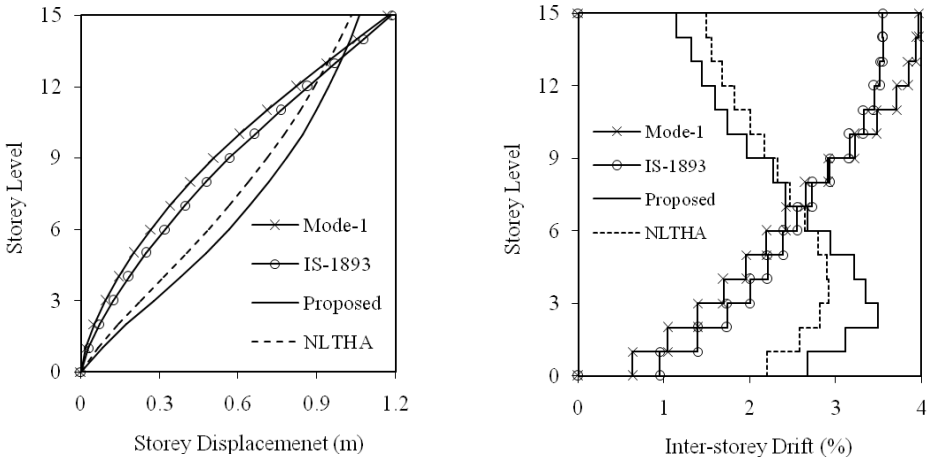

Fig. 19 Displacement and inter-storey drift profile at collapse for a typical stepped frame (S2-15)

the time history analyses. Peak inter-storey drift is considered as the damage parameter in this study and an inter-storey drift of 4% is considered as collapse performance level as per ASCE/SEI 41-13. However, due to early formation of collapse mechanism, the building frame reached 'collapse' for certain cases before the inter-storey drift reaches 4%. The main conclusion from this figure is that the proposed load pattern is able to predict the displacement and drift profile of stepped building better than other existing load patterns. Inter-storey drifts for the upper storeys of stepped building frames are found to be comparatively less as upper storeys attract relatively less force during the earthquake ground motion.

7. Conclusions

Stepped building frames constitute a category of vertical irregularity, whose seismic behaviour has not received adequate attention in existing research and code formulation. In this paper, a detailed study has been carried out to address this shortcoming. The salient conclusions are as follows:

• A lateral load profile, appropriate for stepped building frames, is proposed for use in pushover analysis. This has been validated by nonlinear time history analysis.

• An empirical formula (modification of existing ASCE/SEI 41-13 displacement coefficient method for regular RC framed building) is proposed to estimate the 'target displacement' in stepped building frames. This has similarly been validated by nonlinear time history analysis.

• The pushover analysis of RC stepped frames, incorporating the proposed load profile and 'target displacement' estimation procedure, show consistently good performance in comparison with the existing methods of pushover analysis.

Acknowledgments

The authors gratefully acknowledge the financial support received from Department of Science

and Technology, Govt. of India (Sanction Letter: SR/FRP/ETA-0004/2010) for completion of this work.

References

ASCE 7 (2010), *Minimum Design Loads for Buildings and Other Structures*, American Society of Civil Engineers.

ASCE/SEI 41-13 (2014), *Seismic Evaluation and Retrofit of Existing Buildings*, American Society of Civil Engineers, Reston, Virginia, USA.

ATC 40 (1996), *Seismic Evaluation and Retrofit of Concrete Buildings: Vol. 1*, Applied Technology Council, USA.

Athanassiadou, C.J. (2008), "Seismic performance of R/C plane frames irregular in elevation", *Eng. Struct.*, **30**(5), 1250-1261.

Carvalho, G., Bento, R. and Bhatt, C. (2013), "Nonlinear static and dynamic analyses of reinforced concrete buildings - comparison of different modelling approaches", *Earthq. Struct.*, **4**(5), 451-470.

Cheung, V. and Tso, W. (1987), "Lateral load analysis for buildings with setback", *J. Struct. Eng*., ASCE, **113**(2), 209-227.

Chopra, A.K. and Goel, R.K. (2002), "A modal pushover analysis procedure for estimating seismic demands for buildings", *Earthq. Eng. Struct. Dyn.*, **31**(3), 561-582

Chopra, A.K., Goel, R.K. and Chintanapakdee, C. (2004), "Evaluation of a modified MPA procedure assuming higher modes as elastic to estimate seismic demands", *Earthq. Spectra*, **20**(3), 757-778

Das, S. and Nau, J.M. (2003), "Seismic design aspects of vertically irregular reinforced concrete buildings", *Earthq. Spectra*, **19**(3), 455-477.

Dolšek, M. and Fajfar, P. (2005), "Simplified non-linear seismic analysis of infilled reinforced concrete frames", *Earthq. Eng. Struct. Dyn.*, **34**(1), 49-66.

Elnashai, A. and Sarno, L.D. (2008), *Fundamentals of Earthquake Engineering*, Wiley, New York.

Fahjan, Y. and Ozdemir, Z. (2008), "Scaling of earthquake accelerograms for non-linear dynamic analyses to match the earthquake design spectra", *14th World Conference on Earthquake Engineering*, Beijing, China.

FEMA 356 (2000), *Prestandard and Commentary for the Seismic Rehabilitation of Existing Buildings*, Federal Emergency Management Agency and American Society of Civil Engineers.

Gasparini, D. and Vanmarcke, E. (1976), *SIMQKE - A Program for artificial Motion Generation*, Department of Civil Engineering, Massachusette Institute of Technology, USA.

Goel, R.K. and Chopra, A.K. (1997), "Period formulas for moment resisting frame buildings", *J. Struct. Eng*., ASCE, **123**(11), 1454-1461.

IS 13920 (1993), *Indian Standard Code of Practice for Ductile Detailing of Reinforced Concrete Structures Subjected to Seismic Forces,* Bureau of Indian Standards, New Delhi.

IS 1893 Part 1 (2002), *Indian Standard Criteria for Earthquake Resistant Design of Structures*, Bureau of Indian Standards, New Delhi.

IS 456 (2000), *Indian Standard for Plain and Reinforced Concrete - Code of Practice*, Bureau of Indian Standards, New Delhi.

Jan, T.S., Liu, M.W. and Kao, Y.C. (2004), "An upper-bond pushover analysis procedure for estimating the seismic demands of high-rise buildings", *Eng. Struct.*, **26**(1), 117-128.

Jiang, Y., Li, G. and Yang, D. (2010), "A modified approach of energy balance concept based multimode pushover analysis to estimate seismic demands for buildings", *Eng. Struct.*, **32**(5), 1272-1283.

Karavasilis, T.L., Bazeos, N. and Beskos, D.E. (2008), "Seismic response of plane steel MRF with setbacks: Estimation of inelastic deformation demands", *J. Constr. Steel Res.*, **64**(6), 644-654.

Luca, F.D., Verderame, G.M. and Manfredi, G. (2014), "Eurocode-based seismic assessment of modern heritage RC structures: The case of the Tower of the Nations in Naples (Italy)", *Eng. Struct.*, **74**, 96-110.

Panagiotakos, T.B. and Fardis, M.N. (2001), "Deformation of reinforced concrete members at yielding and ultimate", *ACI Struct. J.*, **98**(2), 135-148.
Papanikolaou, V.K., Elnashai, A.S. and Pareja, J.F. (2005), *Limits of Applicability of Conventional and Adaptive Pushover Analysis for Seismic Response Assessment*, Report of Mid-America Earthquake Center, University of Illinois at Urbana-Champaign.
Paulay, T. and Priestley, M.J.N. (1992), *Seismic Design of Reinforced Concrete and Masonry Buildings*, John Wiley and Sons, New York.
Reyes, J.C., Riaño, A.C., Kalkan, E. and Arango, C.M. (2015), "Extending modal pushover-based scaling procedure for nonlinear response history analysis of multi-story unsymmetric-plan buildings", *Eng. Struct.*, **88**, 125-137.
Roy, R. and Mahato, S. (2013), "Equivalent lateral force method for buildings with setback: adequacy in elastic range", *Earthq. Struct.*, **4**(6), 685-710.
SAP 2000 (2007), *Integrated Software for Structural Analysis and Design* (v.11), Computers & Structures, Inc., Berkeley, California.
Sarkar, P. (2008), "Seismic evaluation of reinforced concrete stepped building frames", Ph.D. Thesis, Indian Institute of Technology Madras, Chennai.
Sarkar, P., Prasad, A.M. and Menon, D. (2010), "Vertical geometric irregularity in stepped building frames", *Eng. Struct.*, **32**(8), 2175-2182.
Sharooz, B.B. and Moehle, J.P. (1990), "Seismic response and design of setback buildings", *J. Struct. Div.*, ASCE, **116**(5), 2002-2014.
Suárez, L.E. and Montejo, L.A. (2005), "Generation of artificial earthquakes via the wavelet transform", *Int. J. Solid. Struct.*, **42**(21-22), 5905-5919.
Vanmarcke, E.H. and Gasparini, D.A. (1976), "Simulated earthquake motions compatible with prescribed response spectra", Report No. R76-4, Department of Civil Engineering, Massachusetts Institute of Technology Cambridge.
Varadharajan, S., Sehgal, V.K. and Saini, B. (2013a), "Seismic behavior of multistory RC building frames with vertical setback irregularity", *Struct. Des. Tall Spec. Build.*, **23**(18), 1345-1380.
Varadharajan, S., Sehgal, V.K. and Saini, B. (2013b), "Determination of inelastic seismic demands of RC moment resisting setback frames", *Archiv. Civ. Mech. Eng.*, **13**(3), 370-393.
Wong, C.M. and Tso, W.K. (1994), "Seismic loading for buildings with setbacks", *Can. J. Civ. Eng.*, **21**(5), 863-871.
Wood, S.L. (1992), "Seismic response of RC frames with irregular profiles", *J. Struct. Eng.*, ASCE, **118**(2), 545-566.

KT